ELSEVIER

Journal of Hazardous Materials B83 (2001) 255–264

Journal of Hazardous Materials

www.elsevier.nl/locate/jhazmat

reference 1

Oxidation of *p*-hydroxybenzoic acid by UV radiation and by TiO_2/UV radiation: comparison and modelling of reaction kinetic

Jesus Beltran De Heredia [a,*], Joaquin Torregrosa [a], Joaquin R. Dominguez [a], Jose A. Peres [b]

[a] *Departamento de Ingenieria Quimica y Energetica, Universidad de Extremadura, 06071 Badajoz, Spain*
[b] *Departamento de Quimica. Universidade de Trás-os-Montes e Alto Douro, 5001 Vila Real, Portugal*

Received 6 January 2001; received in revised form 12 January 2001; accepted 26 February 2001

Abstract

The phenolic compound *p*-hydroxybenzoic acid is very common in a great variety of agroindustrial wastewaters (olive oil and table olive industries, distilleries). The objective of this work was to study the photocatalytic activity of TiO_2 towards the decomposition of *p*-hydroxybenzoic acid. In order to demonstrate the greater oxidizing power of the photocatalytic system and to quantify the additional levels of degradation attained, we performed experiments on the oxidation of *p*-hydroxybenzoic acid by UV radiation alone and by the TiO_2/UV radiation combination. A kinetic model is applied for the photooxidation by UV radiation and by the TiO_2/UV system. Experimental results indicated that the kinetics for both oxidation processes can be fitted well by a pseudo-first-order kinetic model. The second oxidation process can be explained in terms of the Langmuir–Hinshelwood kinetic model. The values of the adsorption equilibrium constant, K_{pHB}, and the second order kinetic rate constant, k_c, were 0.37 ppm^{-1} and 6.99 ppm min^{-1}, respectively. Finally, a comparison between the kinetic rate constants for two oxidation systems reveals that the constants for the TiO_2/UV system are clearly greater (between 220–435%) than those obtained in the direct UV photooxidation.

Keywords: Kinetics; Photocatalysis; *p*-Hydroxybenzoic acid; Titanium dioxide; UV radiation

Phenols, e.g., p-hydroxybenzoic acid, are contained in the agroinductrial (olive oil, wine ...) waste water.

---> photocatalytic oxidative decomposition under UV irradiation

1. Introduction

Industries of olive oil extraction, table olive production, and alcohol distillation from different wine fractions give rise to highly contaminant wastewaters. This is a major envi-

* Corresponding author. Fax: +34-924-271304.
E-mail address: jbelther@unex.es (J.B. De Heredia).

0304-3894/01/$ – see front matter
PII: S0304-3894(01)00194-7

ronmental problem in Mediterranean countries in general, and particularly in certain areas of Spain and Portugal where there are many small plants.

Most of these wastewaters pollutant properties have been imputed to phenolic compounds, because of their toxicity [1] and power to inhibit biological treatments [2]. As a consequence of this situation and the more stringent regulations concerning effluents released into public rivers and streams, new technologies have been developed to reduce these refractory contaminants. Among them, chemical oxidations [3,4] are increasingly used for the reduction of organic contaminants present in a variety of wastewaters from different industrial plants. However, this decomposition using single treatments may sometimes be difficult if the pollutants are present at low concentrations or if they are especially refractory to the oxidants. For such situations, it has been necessary to develop more effective processes for the destruction of the contaminants.

hydroxyl radical has strong oxidative power ---> AOPs (including TiO2 photocatalysis?)

For example, systems based on the generation of very reactive oxidizing free radicals, especially hydroxyl radicals, have generated increasing interest due to their high oxidant power (+2.8 V). These systems are commonly termed Advanced Oxidation Processes (AOPs). The radicals are produced by combinations of ozone, hydrogen peroxide, UV radiation [5–7] and photocatalysts [8–11]. These methods can provide almost total degradation as has been reported by several authors for the decomposition of a wide variety of organic contaminants [4,12,13].

The objective was to study the decomposition of *p*-hydroxybenzoic acid in aqueous solution by UV radiation alone and by the combination titanium dioxide/UV radiation.

2. Experimental section

The experiments were carried out in a 500 ml cylindrical glass jacketed photochemical reactor, charged with 350 ml of aqueous solution of *p*-hydroxybenzoic acid (Fig. 1). The reactor was equipped with an ultraviolet lamp, located axially and held in a quartz sleeve. The radiation source was a Heraeus TQ-150 medium pressure mercury vapor lamp which emits polychromatic radiation in the range from 185 to 436 nm. A porous plate was placed at the reactor bottom below the quartz sleeve to provide some agitation through bubbling during experiments. In order to carry out all the experiments always under aerobic conditions, the dispersion was saturated by bubbling oxygen at atmospheric pressure, before starting the irradiation, during the runs also an oxygen flow rate of 40 l/h was continuously bubbled into the dispersion. Water from a thermostatic bath was circulated through the reactor jacket to ensure a constant temperature of $20 \pm 0.5^{\circ}C$ inside the reactor.

Two experimental series were carried out to study the photolytic and photocatalytic decomposition of *p*-hydroxybenzoic acid. In the direct photolytic series, the variable modified was the initial organic compound concentration, and in the photocatalytic series was also modified the photocatalyst concentration. This series was carried out using 0.5 g/l suspensions of TiO_2. Aqueous suspensions of TiO_2 containing *p*-hydroxybenzoic acid were sonicated for 15 min before illumination, to make the TiO_2 particle size uniform. During the experiments, samples were withdrawn regularly from the reactor for analysis. The quantitative determination of *p*-hydroxybenzoic acid was performed, after separation of the catalyst

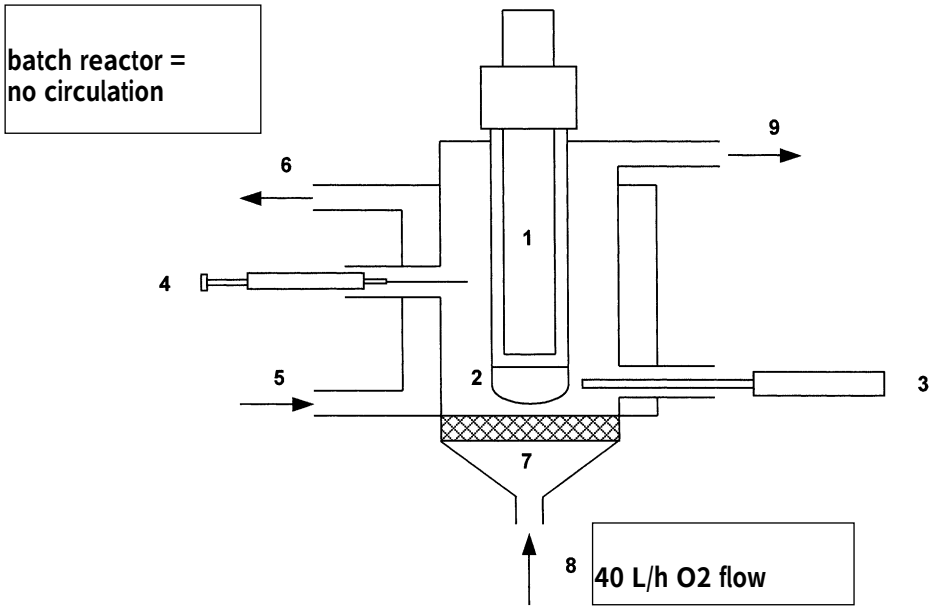

Fig. 1. Experimental photochemical reactor. 1: Medium pressure mercury vapor lamp; 2: quartz sleeve; 3: temperature measuring device; 4: sampling point; 5: cooling water flow inlet; 6: cooling water flow outlet; 7: porous plate; 8: oxygen flow inlet; 9: oxygen flow outlet.

(if it was necessary) by a 0.45 μm Millipore filter, by HPLC using a Waters chromatograph equipped with a 996 photodiode array detector and a Nova-Pack C-18 column. Detection was at 254 nm with a mobile phase composed of a methanol:water:acetic acid mixture (10:88:2 in volume) at a flow rate of 1 ml/min.

only p-hydroxybenzoic acid (pHB) was measured by HPLS (no detection of CO2 etc)

Analytical grade *p*-hydroxybenzoic acid was obtained from Sigma, titanium dioxide (Degussa P-25) from Degussa Portugal.

In order to determine the power emitted by the radiation source, several experiments were carried out with an actinometric system at the same experimental conditions. In this work, the uranyloxalate actinometry was used, which consists in the photochemical decomposition of aqueous solutions of oxalic acid in the presence of uranyl salts [14,15]. The power emitted by the lamp was deduced, its value being 3.30×10^{-5} einstein/s [16].

no description on the wavelength for actinometry
(wavelength dependence of uranyloxalate actinometry

3. Results and discussion

3.1. Photolytic oxidation by UV radiation

Several experiments of individual *p*-hydroxybenzoic acid photodecomposition were performed. In this case the oxidizing agent is only the polychromatic UV radiation emitted by the radiation source described in the experimental section.

From an observation of the degradation curves of *p*-hydroxybenzoic acid by UV radiation, it can be deduced that the elimination of the said phenolic acid fulfils the conditions established for a first-order homogeneous reaction kinetic model. Such a simplified model has been used previously by various researches for the present system of UV radiation. By means of the present model one can carry out a simplified kinetic study of the process and calculate the first-order kinetic rate constants. The objective of its application is to be able to determine the said reaction rate constants and compare them with those obtained in other more complex oxidation systems, such as the TiO_2/UV combination. Thus, on comparing the values of the first-order constants obtained in the two processes, one will be able to compare their efficacy. Applying the above model to the simple photodegradation system, one obtains the following kinetic Eq. (1):

$$-\frac{\mathrm{d[pHB]}}{\mathrm{d}t} = k_{\mathrm{UV}}[\mathrm{pHB}] \tag{1}$$

which integrated from $t = 0$ to $t = t$ becomes

$$\ln\left(\frac{[\mathrm{pHB}]_0}{[\mathrm{pHB}]}\right) = k_{\mathrm{UV}}t \tag{2}$$

According to this Eq. (2), a plot of the first term against the reaction time should be a straight line of slope k_{UV}. Photodegradation experiments using UV radiation modifying the initial *p*-hydroxybenzoic acid concentration (50, 25, 10, 5 and 2.5 ppm) are showed in Table 1. It can be seen the conversions achieved in the *p*-hydroxybenzoic acid degradation at the reference time of 5 min (X_5). The slopes, k_{UV}, clearly increase where the acid concentration decreases. This fact is attributable to the increase of the number of photons per organic molecule.

3.2. Photocatalytic oxidation over TiO_2

In the oxidation experiments with TiO_2, photoexcitation with light of an energy greater than the TiO_2 band gap promotes an electron from the valence band to the conduction band, and leaves an electronic vacancy or hole (h^+) in the valence band. Thus the act of photoexcitation generates an electron-hole pair

$$TiO_2 \xrightarrow{h\nu} TiO_2(h^+ + e^-) \tag{3}$$

Table 1
p-Hydroxybenzoic acid conversion (at 5 min) and pseudo-first-order kinetic rate constants in UV experiments with different initial concentration

Experiment	$[\mathrm{pHB}]_0$ (ppm)	X_5 (%)	k_{UV} (min^{-1})
U-1	50	20	0.05
U-2	25	24	0.11
U-3	10	42	0.21
U-4	5	70	0.27
U-5	2.5	72	0.28

without TiO2 = UV irradiation only

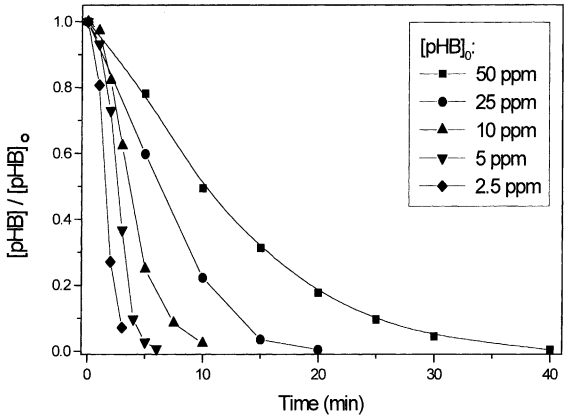

Fig. 2. Evolution of $[pHB]/[pHB]_0$ vs. time for all the experiments where the initial concentration of *p*-hydroxybenzoic acid was varied.

In order to achieve chemically productive photocatalysis, electron-hole pair recombination must be suppressed. This can be achieved by "trapping" these species with the surface adsorbates. The photo-excited electrons are trapped by molecular oxygen

$$e^- + O_2(\text{ads.}) \rightarrow O_2{}^-(\text{ads.}) \quad (4)$$

The principal hole traps are adsorbed water molecules and OH^- ions [17,18] producing $OH^\bullet$ radicals

$$h^+ + H_2O(\text{ads.}) \rightarrow OH^\bullet(\text{ads.}) + H^+ \quad (5)$$

$$h^+ + OH^- \rightarrow OH^\bullet(\text{ads.}) \quad (6)$$

Fig. 2, shows a plot of $[pHB]/[pHB]_0$ versus time for all the experiments of photocatalytic decomposition where the initial concentration of *p*-hydroxybenzoic acid was varied. The initial *p*-hydroxybenzoic acid concentration has a pronounced effect on the degradation rate, at the same illumination time the percentage of *p*-hydroxybenzoic acid decomposed is smaller if the initial *p*-hydroxybenzoic acid concentration is higher (Table 2).

Table 2
p-Hydroxybenzoic acid conversion (at 5 min) and pseudo-first-order kinetic rate constants in photocatalytic experiments with different initial concentration

Experiment	TiO_2 (ppm)	$[pHB]_0$ (ppm)	X_5 (%)	k_{obs} (min^{-1})	$1/k_{obs}$ (min)
T-1	500	50	21.8	0.13	7.63
T-2	500	25	40.2	0.27	3.65
T-3	500	10	75.1	0.46	2.16
T-4	500	5	97.2	1.16	0.86
T-5	500	2.5	100	1.20	0.82

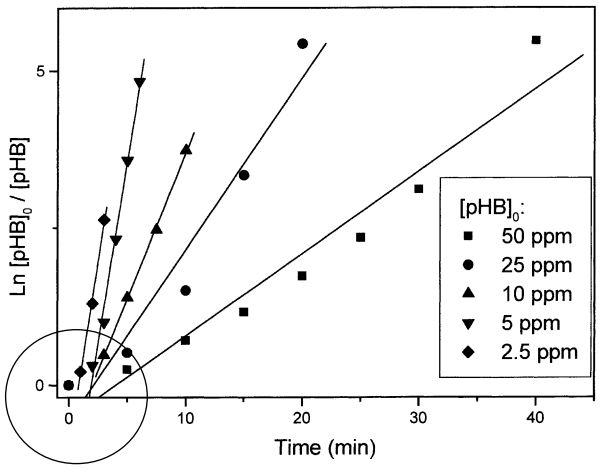

all lines "must" be "0" at time 0, since [pHB] = [pHB]0

Fig. 3. Determination of the pseudo-first-order kinetic rate constant, k_{obs}.

--> Table 2

Degradation experiments of *p*-hydroxybenzoic acid by UV radiation in the presence of TiO_2 also exhibited pseudo-first-order kinetics with respect to the concentration of the organic compound

$$-\frac{d[pHB]}{dt} = k_{obs}[pHB] \tag{7}$$

whose integration gives, for $[pHB] = [pHB]_0$ at $t = 0$:

$$\ln\left(\frac{[pHB]_0}{[pHB]}\right) = k_{obs}t \tag{8}$$

in which [pHB] is the *p*-hydroxybenzoic acid concentration at time *t*, $[pHB]_0$ is the *p*-hydroxybenzoic acid concentration at initial time, *t* the reaction time and k_{obs} the pseudo-first-order rate constant.

Fig. 3, shows a plot of $\ln([pHB]_0/[pHB])$ versus time for all the experiments with different initial concentration of phenolic acid. By applying a least square regression analysis the values of k_{obs} have been obtained. Table 2 reports the values of k_{obs} for all experiments carried out. The reaction rate proceeds according to pseudo-first-order kinetics with a kinetic constant, which decreases as the initial reactant concentration.

On the basis of all the previous considerations, a chemical kinetic model is proposed, able to explain the experimental results. The rate determining step of the catalysed reaction is considered to be the reaction between $OH^{\bullet}$ radicals and organic molecules over the catalyst surface.

It is well known that the titania surface possesses both acidic and basic sites. The acidic sites are associated with coordinatively unsaturated surface metal ions while the latter are associated with surface anions or anion vacancies. Two different types of surface sites are hypothesised to be involved in the adsorption processes of the reacting species. The first are able to adsorb *p*-hydroxybenzoic molecules and their degradation products. The second

assuming two different kind of adsorption site; one for pHB and degradation intermediates and the others for O2

assuming the rate of photocatalytic reaction is dominated by the surface reaction of e or h with adsorbed species, but not diffusion of substrates or O2

are able to adsorb oxygen. In this hypothesis the reaction rate for second order surface decomposition of *p*-hydroxybenzoic acid may be written in terms of Langmuir–Hinshelwood kinetics as:

$$r = k'' \Theta_{OH} \Theta_{pHB} \tag{9}$$

in which k'' is the surface second order rate constant, Θ_{OH} the fractional site coverage by hydroxyl radicals and Θ_{pHB} the fraction of sites covered by *p*-hydroxybenzoic acid. These two last variables can be written in the following way:

$$\Theta_{OH} = \frac{K_{O_2} P_{O_2}}{1 + K_{O_2} P_{O_2}} \tag{10}$$

$$\Theta_{pHB} = \frac{K_{pHB}[pHB]}{1 + K_{pHB}[pHB] + \sum_i K_i [I_i]} \tag{11}$$

in which K_{o_2}, K_{pHB} and K_i are equilibrium adsorption constants and 'I' refers to the various intermediate products of *p*-hydroxybenzoic acid degradation. Eq. (11) contains several unknown factors, but can be modified by making the following assumption:

$$K_{pHB}[pHB] + \sum_i K_i [I_i] = K_{pHB}[pHB]_0 \tag{12}$$

where $[pHB]_0$ is the initial concentration of *p*-hydroxybenzoic acid. The assumption is that the adsorption coefficients for all organic molecules present in the reacting mixture are effectively equal. Substitution of Eq. (12) into Eq. (11) produces the expression

$$r = k'' \frac{K_{O_2} P_{O_2}}{1 + K_{O_2} P_{O_2}} \frac{K_{pHB}[pHB]}{1 + K_{pHB}[pHB]_0} \tag{13}$$

Owing to the fact that the oxygen partial pressure remained constant for all the photocatalytic runs, the fractional site coverage by hydroxyl radicals was also constant

$$k'' \frac{K_{O_2} P_{O_2}}{1 + K_{O_2} P_{O_2}} = \text{constant} = k_c \tag{14}$$

Eq. (13) can therefore be written as:

$$r = k_c \frac{K_{pHB}[pHB]}{1 + K_{pHB}[pHB]_0} = k_{obs}[pHB] \tag{15}$$

that is a first-order kinetic equation with respect to organic concentration. The relationship between k_{obs} and $[pHB]_0$ can be expressed as a linear Eq. (16).

$$\frac{1}{k_{obs}} = \frac{1}{k_c K_{pHB}} + \frac{[pHB]_0}{k_c} \tag{16}$$

The data reported in Table 2 are plotted in Fig. 4 as $1/k_{obs}$ versus $[pHB]_0$. By means of a least square best fitting procedure, the values of the adsorption equilibrium constant, K_{pHB}, and the second order rate constant, k_c. The values were $K_{pHB} = 0.37\,\text{ppm}^{-1}$ and $k_c = 6.99\,\text{ppm min}^{-1}$.

assuming pHB -> (intermediate A) -> (B) -> ->-> final product, and the properties (adsorption and oxidation) of these intermediates are same as those of pHB

cf. usually the more degraded, the faster reacts, suggested by the upward curvature in Figure 3

--> Figure 4 [a linear line was obtained]

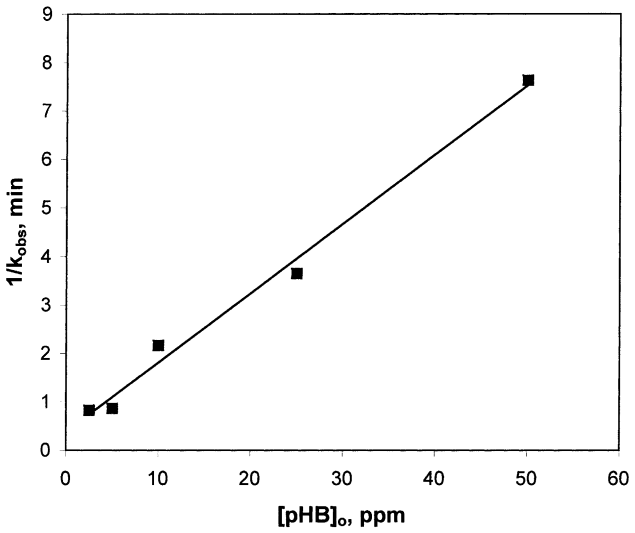

Fig. 4. Determination of the adsorption equilibrium constant, K_{pHB}, and the second order rate constant, k_c for the Langmuir–Hinshelwood kinetic model

Fig. 5, shows a comparison between the kinetic rate constants for two oxidation systems. As can be seen, the values of the constants for the TiO_2/UV system are clearly greater than those obtained in the direct UV photooxidation. The difference clearly increase where the phenolic acid concentration decreases. This fact is attributable to the major catalytic effect because the increase of the relationship active sites per organic molecule.

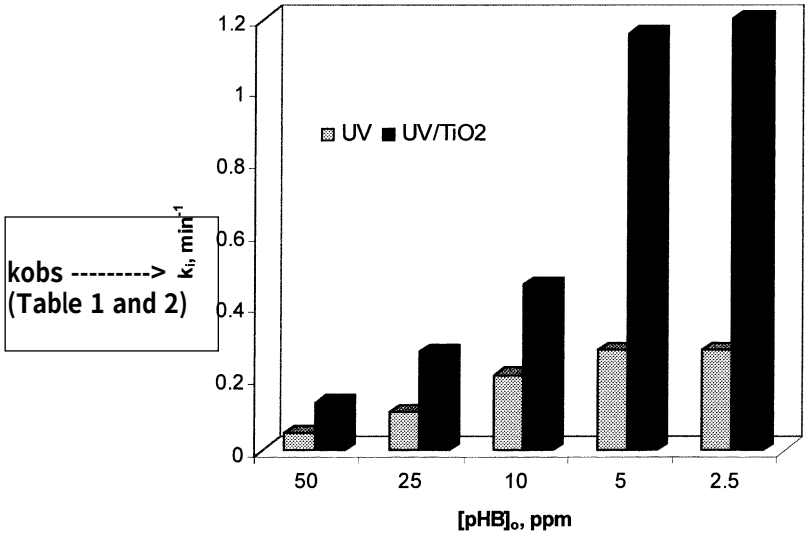

Fig. 5. Comparison between the pseudo-first-order kinetic rate constants for UV radiation and TiO_2/UV radiation processes.

4. Conclusions

The effectiveness of the photocatalytic process using TiO_2 in the degradation of *p*-hydroxybenzoic acid has been demonstrated and the kinetics of reaction has been determined. The experimental results indicated that the kinetics for both oxidation processes, UV radiation and TiO_2/UV radiation, fit well a pseudo-first-order kinetic model. The photocatalytic degradation process of *p*-hydroxybenzoic acid can be explained in terms of the Langmuir–Hinshelwood kinetic model. Experiments using various concentrations of *p*-hydroxybenzoic acid showed that the more diluted the initial solution, the faster is the *p*-hydroxybenzoic acid degradation. This fact is attributable to the increase of the relationship active sites per organic molecule. The values of the adsorption equilibrium constant, K_{pHB}, and the second order rate constant, k_c, were $0.37\,ppm^{-1}$ and $6.99\,ppm\,min^{-1}$, respectively.

Finally, a comparison between the kinetic rate constants for two oxidation systems reveals that the constants for the TiO_2/UV system are clearly greater (between 220–435%) than those obtained in the direct UV photooxidation.

Acknowledgements

This research has been supported by the "Comision Interministerial de Ciencia y Tecnologia'' (CICYT) of Spain, under Project AMB 97-0339 and by the Junta de Extremadura, under Project IPR 98A014. Joaquin R. Dominguez Vargas wishes to thank Ministerio de Educacion y Cultura for the financial support to his Ph.D. Grant.

References

[1] N. Zouari, R. Ellouz, Toxic effect of coloured olive compounds on the anaerobic digestion of olive oil mill effluent in UASB-like reactors., J. Chem. Technol. Biotechnol. 66 (4) (1996) 414–420.
[2] R. Borja, A. Martin, R. Maestro, M. Luque, M.M. Duran, Enhancement of the anaerobic digestion of wine distillery wastewater by the removal of phenolic inhibitors, Bioresourc. Technol. 45 (2) (1993) 99–104.
[3] O. Legrini, E. Oliveros, A.M. Braun, Photochemical processes for water treatment, Chem. Rev. 93 (2) (1993) 671–698.
[4] R.G. Rice, Applications of ozone for industrial wastewater treatment. A review, Ozone Sci. Eng. 18 (6) (1996) 477–515.
[5] G. Ruppert, R. Bauer, G. Heisler, UV-O_3, UV-H_2O_2, UV-TiO_2 and the photo-Fenton reaction: comparison of advanced oxidation processes for wastewater treatment, Chemosphere 28 (8) (1994) 1447–1454.
[6] R. Andreozzi, Advanced oxidation processes (AOP) for water purification and recovery, Catal. Today 53 (1) (1999) 51–59.
[7] F.J. Benitez, J. Beltran-Heredia, J.L. Acero, F.J. Rubio, Contribution of free radicals to chlorophenols decomposition by several advanced oxidation processes, Chemosphere 41 (8) (2000) 1271–1277.
[8] A. Mills, S.L. Hunte, An overview of semiconductor photocatalysis, J. Photochem. Photobiol. A 108 (1) (1997) 1–35.
[9] S. Malato, J. Blanco, C. Richter, B. Braun, M.I. Maldonado, Enhancement of the rate of solar photocatalytic mineralization of organic pollutants by inorganic oxidizing species, Appl. Catal. B 17 (4) (1998) 347–356.
[10] J.M. Herrmann, Heterogeneous photocatalysis: fundamentals and applications to the removal of various types of aqueous pollutants, Catal. Today 53 (1) (1999) 115–129.

[11] M.I. Litter, Heterogeneous photocatalysis. Transition metal ions in photocatalytic systems, Appl. Catal. B 23 (2-3) (1999) 89–114.
[12] W.S. Kuo, Synergistic effects of combination of photolysis and ozonation on destruction of chlorophenols in water, Chemosphere 39 (11) (1999) 1853–1860.
[13] J. de Laat, H. Gallard, S. Ancelin, B. Legube, Comparative study of the oxidation of atrazine and acetone by H_2O_2/UV, Fe(III)/UV, Fe(III)/H_2O_2/UV and Fe(II) or Fe(III)/H_2O_2, Chemosphere 39 (15) (1999) 2693–2706.
[14] D.H. Volman, J.R. Seed, The photochemistry of uranyl oxalate, J. Am. Chem. Soc. 86 (23) (1964) 5095–5098.
[15] L.J. Heidt, G.W. Tregay, F.A. Middleton, Influence of pH upon the photolysis of uranyl oxalate actinometer system, J. Phys. Chem. 74 (9) (1970) 1876–1882.
[16] J. Beltran-Heredia, J. Torregrosa, J.R. Dominguez, J.A. Peres, Comparison of several oxidation processes for the decomposition of *p*-hydroxybenzoic acid, Chemosphere 42 (4) (2001) 351–359.
[17] M.A. Fox, M.T. Dulay, Heterogeneous photocatalysis, Chem. Rev. 93 (1) (1993) 341–357.
[18] M.R. Hoffmann, S.T. Martin, W. Choi, D.W. Bahnemann, Environmental applications of semiconductor photocatalysis, Chem. Rev. 95 (1) (1995) 69–96.

ELSEVIER

Catalysis Today 66 (2001) 475–485

CATALYSIS TODAY

www.elsevier.com/locate/cattod

reference 2

External and internal mass transfer effect on photocatalytic degradation

Dingwang Chen, Fengmei Li, Ajay K. Ray*

Department of Chemical and Environmental Engineering, The National University of Singapore, 10 Kent Ridge Crescent, Singapore 119260, Singapore

Abstract

A rational approach is proposed in determining the effect of internal and external mass transfer, and catalyst layer thickness during photocatalytic degradation. The reaction occurs at the liquid–catalyst interface and therefore, when the catalyst is immobilized, both external and internal mass transfer plays significant roles in overall photocatalytic processes. Several model parameters, namely, external mass transfer coefficient, dynamic adsorption equilibrium constant, adsorption rate constant, internal mass transfer coefficient, and effective diffusivity were determined either experimentally or by fitting realistic models to experimental results using benzoic acid as a model component. The effect of the internal mass transfer on the photocatalytic degradation rate over different catalyst layer thickness under two different illuminating configurations was analyzed theoretically and later experimentally verified. It was observed that an optimal catalyst layer thickness exists for SC (substrate-to-catalyst) illumination.

Keywords: Photocatalysis; Mass transfer; Catalyst layer thickness; TiO_2; Water purification; Kinetic study

1. Introduction

Semiconductor photocatalytic processes have been studied for nearly 20 years due to their intriguing advantages in environmental remediation. Among the semiconductor photocatalysts tested, Degussa P25 TiO_2 has been proven to be the most active catalyst. TiO_2 catalyst has been used in two forms: suspended in aqueous solutions in the form of slurry, and immobilized onto rigid inert supports. In the former case, a high ratio of illuminated surface of catalyst to the effective reactor volume can be achieved for small well-designed photocatalytic reactor [1] and almost no mass transfer limitation exists since the maximum diffusional distance is very small resulting from the use of ultra-fine (<30 nm) catalyst particles [2]. However, in large-scale applications, the catalyst particles must be filtered prior to the discharge of the treated water, even though TiO_2 is harmless to environment. Besides, the penetration depth of UV light is limited due to the strong absorption by TiO_2 and dissolved organic species. All these disadvantages render the scale-up of a slurry photocatalytic reactor difficult [3,4].

Above problems can be eliminated by immobilizing TiO_2 catalyst over suitable supports [5]. Design and development of immobilized thin catalyst film makes it possible for commercial-scale applications of TiO_2 based photocatalytic processes for water treatment [6,7]. The designs are more likely to be useful in commercial applications as it provides at least three important advantages. Firstly, it eliminates the need for separation of catalyst particles from treated liquid and enables the contaminated water to be treated continuously. Secondly, the catalyst film is porous,

* Corresponding author. Tel.: +65-874-8049; fax: +65-779-1936.
E-mail address: cheakr@nus.edu.sg (A.K. Ray).

0920-5861/01/$ – see front matter
PII: S0920-5861(01)00256-5

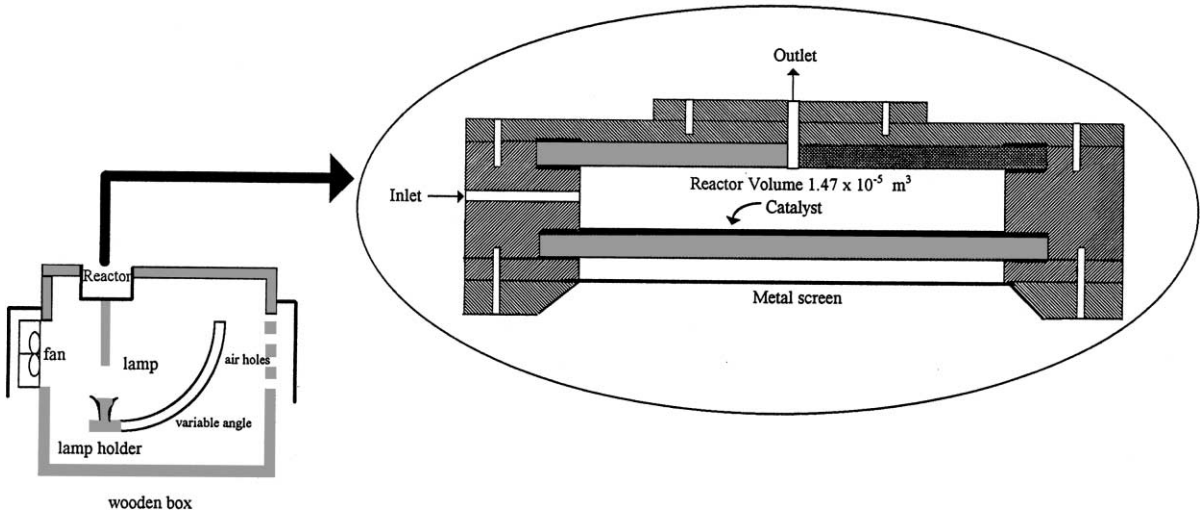

Fig. 1. Schematic diagram of the kinetic reactor.

reaction samples was analyzed by a HPLC (Perkin Elmer LC240). Aliquots of 20 μl were injected onto a reverse-phase C-18 column (Chrompack), and eluted with the mixture of acetonitrile (60%) and ultrapure water (40%) at a total flow rate of 1.5 ml/min. Absorbance at 229 nm was used to measure the concentration of above compounds by a UV/VIS detector (Perkin Elmer 785A). All water samples were filtered by Millex–HA filter (Millipore, 0.45 μm) before analyses. The light intensity was measured by a digital radiometer (UVP model number UVX-36).

In this study, circular Pyrex glass (thickness 0.0032 m) was used as catalyst support. Varied thickness of catalyst film was obtained by controlling the speed of coating and number of times coated using an automated dip-coating apparatus [6]. Subsequently, the coated glass plate was calcined in a furnace. The influence of calcination temperature on reactivity of immobilized catalyst layer was reported in one of our earlier paper [11]. The optimal calcination temperature found out was around 573 K. The total mass of catalyst deposited per unit area was determined by weighing the glass plate before and after the catalyst coating. Subsequently, catalyst layer thickness was calculated based on the density of the catalyst particles and layer porosity. Surface texture measurement of the coated catalyst layer by Taylor–Hobson indicated that catalyst particles were uniformly distributed on the entire glass plate. Scanning electron micrograph pictures illustrating the surface morphology of a roughened (sand blasted) glass plate with no catalyst, and TiO_2 films containing 5.0×10^{-4} kg/m^2 (thin film) and 3.0×10^{-3} kg/m^2 (thick film) has been published elsewhere [1]. The coated catalyst was observed to be stable for a wide range of pH. The TiO_2 immobilized in this way was found to be photocatalytically active, capable of decomposing a variety of organic substances including phenol, 4-chlorophenol, 4-nitrophenol and benzoic acid [2,11].

3. Results and discussions

Experiments were performed to study the photocatalytic degradation rate when catalyst was immobilized either on the bottom plate or on the top plate. In the latter case, light intensity on the catalyst surface is considerably reduced, as it travels through the absorbing liquid medium. The two circumstances can be depicted as SC (substrate–catalyst) and LC (liquid–catalyst) illumination [1]. Fig. 2(a) and (b) represent the cases in which the catalyst-coated glass plate is placed at the top (LC illumination) or at the bottom (SC illumination) respectively for the photocatalytic reactor used in this work.

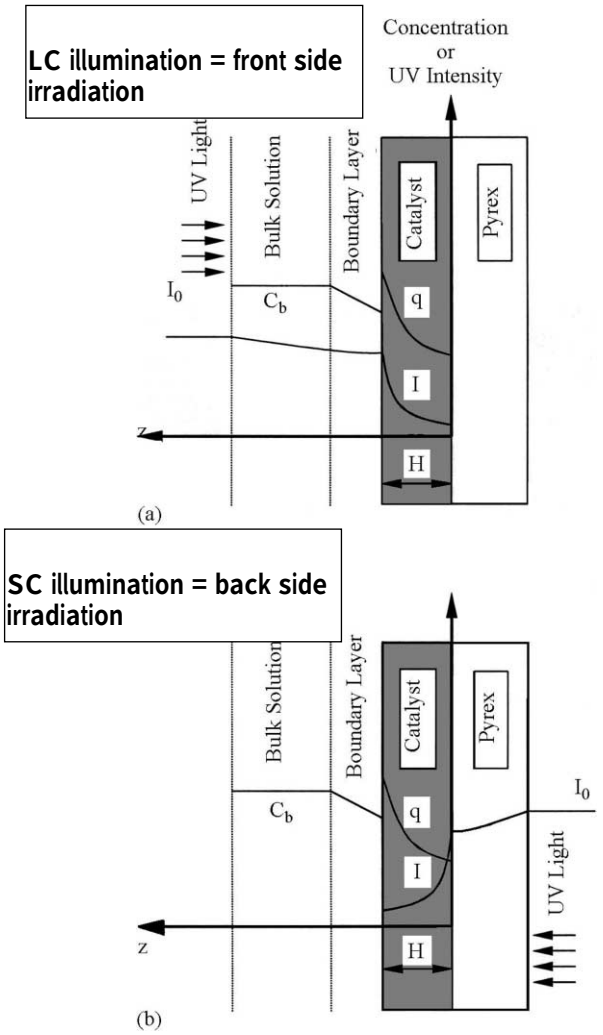

Fig. 2. Schematic diagram of the profiles of concentration and UV light intensity in TiO_2 immobilized system. (a) LC illumination and (b) SC illumination.

In the photocatalytic reaction over immobilized catalyst, both internal and external mass transfer must be considered. The relationship among the observed degradation rate, the external and internal mass transfer rates and the intrinsic kinetic reaction rate are given by the following expression:

$$\left[\frac{1}{k_{\text{obs}}}\right] = \left[\frac{1}{k_{\text{rxn}}}\right] + \left[\frac{1}{k_{\text{m,int}}}\right] + \left[\frac{1}{k_{\text{m,ext}}}\right] \quad (1)$$

In determining the intrinsic kinetic parameters, it is essential to estimate the external mass transfer resistance. At steady state, the mass transfer rate to the catalyst surface, $r_{\text{m,ext}}$, must be equal to the surface catalyzed reaction rate, r_{rxn}: $k_{\text{m,ext}}(C_{\text{b}} - C_{\text{s}}) = k_{\text{rxn}} f(C_{\text{s}})$, where $f(C_{\text{s}})$ represents the concentration dependence of the surface catalyzed reaction rate. The external mass transfer coefficient was determined experimentally by measuring the dissolution rate of benzoic acid into water flowing at different flow rates. The result is shown as a function of Reynolds number in Fig. 3 together with the best least square fit, which is correlated by $k_{\text{m,ext}}(\text{in m/s}) = 3.49 \times 10^{-7} Re^{0.77}$.

The internal mass transfer resistance results from the diffusion of organic molecules within the porous catalyst thin film. Influence of the internal mass transfer can be stipulated by the magnitude of Thiele modulus. Assuming the thin catalyst film as a porous slab, the Thiele modulus is defined as: $\phi_H = H[k_{\text{v}}/D_{\text{e}}]^{1/2}$, for the first order reaction. k_{v} can be determined experimentally by kinetic study at high circulating flow rate over a monolayer of catalyst film. Evidently, effective diffusivity dominates the internal mass transfer process. However, no literature value of effective diffusivity has been reported for organic compounds in porous TiO_2 film. Hence, in this study, the effective diffusivity was determined experimentally. In order to obtain the effective diffusivity, adsorption rate constant, K, need to be first determined by performing the dynamic physical adsorption experiments. The thinnest catalyst film (about 0.63 μm) was used so that the internal mass transfer resistance can be assumed to be negligible. The physical adsorption (dark reaction) process of benzoic acid over a thin TiO_2 catalyst film can be described by the following equations:

$$v\left[\frac{\mathrm{d}C_{\text{b}}}{\mathrm{d}t}\right] = -k_{\text{m,ext}} A(C_{\text{b}} - C_{\text{s}}), \quad \text{at } t = 0,\ C_{\text{b}} = C_0 \quad (2)$$

$$\frac{\mathrm{d}q}{\mathrm{d}t} = K\left[\frac{k_{\text{a}} q_{\text{s}} C_{\text{s}}}{(1 + k_{\text{a}} C_{\text{s}})} - q\right], \quad \text{at } t = 0,\ q = 0 \quad (3)$$

$$v(C_0 - C_{\text{b}}) = mq \quad (4)$$

Rearranging Eqs. (2)–(4) with the assumption that $k_{\text{a}} C_{\text{s}} \ll 1$ at low pollutant concentration, the variation of the bulk concentration of benzoic acid with the adsorption time is

(several pages are deleted)

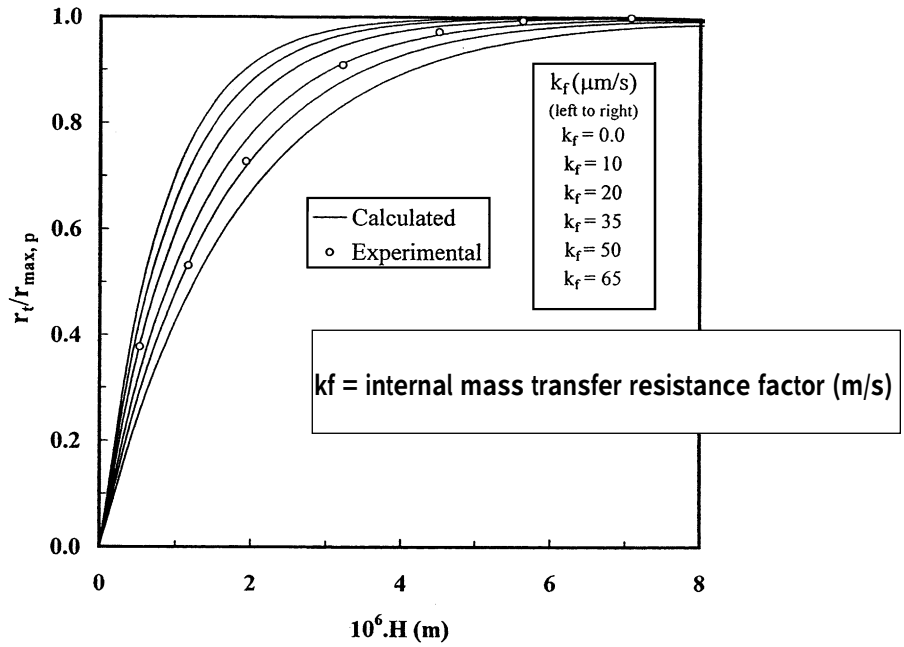

Fig. 8. Experimental determination of k_f for LC illumination ($a = 0.89$, $\alpha = 6.3 \times 10^5\,m^{-1}$, $D_e = 1.0 \times 10^{-10}\,m^2/s$, $A = 0.002\,m^2$, $T = 303\,K$, $v = 1.45 \times 10^{-4}\,m^3$ and $Re = 427$).

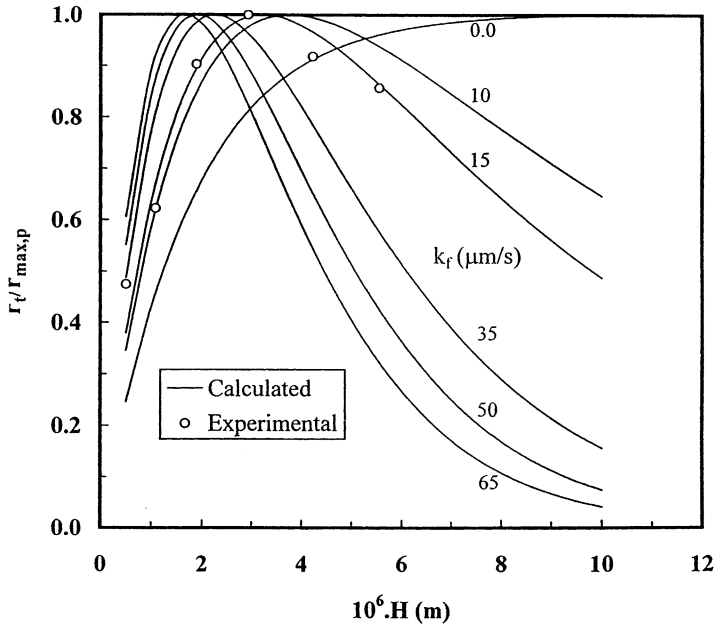

Fig. 9. Experimental determination of k_f for SC illumination ($a = 0.89$, $\alpha = 6.3 \times 10^5\,m^{-1}$, $D_e = 1.0 \times 10^{-10}\,m^2/s$, $A = 0.002\,m^2$, $T = 303\,K$, $v = 1.45 \times 10^{-4}\,m^3$ and $Re = 427$).

(several pages are deleted)

ELSEVIER

Catalysis Today 66 (2001) 487–494

CATALYSIS TODAY

www.elsevier.com/locate/cattod

reference 3

Comparison of the efficiency of immobilized and suspended systems in photocatalytic degradation

M.F.J. Dijkstra*, A. Michorius, H. Buwalda, H.J. Panneman, J.G.M. Winkelman, A.A.C.M. Beenackers

Department of Chemical Engineering, University of Groningen, Nijenborgh 4, 9747 AG, Groningen, The Netherlands

Abstract

The photocatalytic degradation of formic acid in suspended and immobilized systems, with and without oxygen addition, are compared. In the immobilized system, oxygen addition to the reactor appeared to increase the efficiency, not only because oxygen acts as an efficient electron scavenger, but also due to increased mass transfer in this two-phase reactor. This immobilized system had an efficiency comparable to that of the suspended system. The addition of oxygen to the immobilized system appeared to increase the quantum yield with a factor 4, whereas the addition of oxygen to the suspended system hardly had any effect.

Keywords: Photocatalysis; Water purification; Quantum yield

1. Introduction

The purification of wastewater from toxic substances has become a major concern. Quality criteria for both surface water and drinking water tend to become more and more severe with time. In order to cope with these growing demands, new water purification methods are investigated [1,2]. Heterogeneous photocatalysis appears to be a promising novel technique. In this advanced oxidation process almost any organic contaminant can be completely degraded to carbon dioxide, water and mineral acids [3]. This complete destruction of the contaminants is a major advantage of heterogeneous photocatalysis, because no polluted phase remains after the purification as opposed to phase transfer methods (e.g. air stripping, adsorption on activated carbon) [4].

Advanced oxidation processes involve strongly oxidizing hydroxyl radicals, which degrade the pollutants. In heterogeneous photocatalysis, hydroxyl radicals are also assumed to be the reactive species [2,5]. The catalyst in this process is a semiconductor (mostly titanium dioxide) which is activated with near UV light. When a photon with an energy equal to or exceeding the band gap energy of the semiconductor ($h\upsilon \geq E_{gap}$) reaches the surface, an electron (e^-_{cb}) is promoted from the valence band to the conduction band. At the valence edge an electronic vacancy or hole (h^+_{vb}) is created. Both energy carriers can participate in various reactions: the holes and electrons can recombine and the energy will be lost as heat; they can get trapped in metastable surface states; and they can migrate to the surface of the semiconductor and participate in redox reactions with electron donors and electron acceptors adsorbed at the surface [2,6].

To prevent the electron–hole recombination, a suitable scavenger or surface defect state must be available to trap the electron or hole. Howe and Grätzel

* Corresponding author.
E-mail address: m.f.j.dijkstra@chem.rug.nl (M.F.J. Dijkstra).

0920-5861/01/$ – see front matter
PII: S0920-5861(01)00257-7

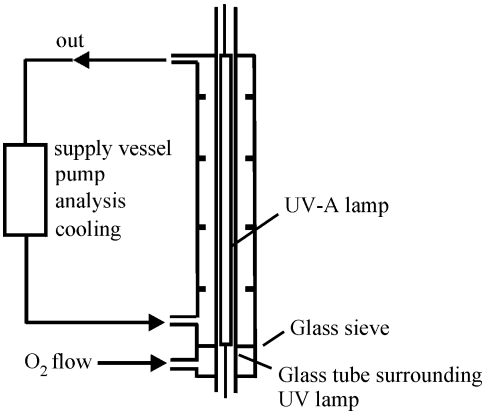

Fig. 1. Scheme of experimental set-up.

transfer characteristics and the quantum yield. From the results, conclusions for the development of an optimal reactor design will be drawn.

2. Experimental methods

2.1. Equipment

The experiments with suspended and the immobilized catalysts were performed in the same reactor to be able to compare the performances accurately. The reactor is a 124×10^{-6} m^3 double wall tubular reactor of borosilicate glass, see Fig. 1. The liquid was fed tangentially into the reactor and baffles were present in the reactor to reduce possible mass transfer limitations. The experiments were performed in a recirculating batch system consisting of a pump, cooling device, reactor vessel and a supply vessel. Cooling was provided by a Tamson 1000 thermostatic bath. In the inner tube a Philips TL29D15/09 (Cleo 15 W) UV-A lamp was placed. The total UV-A radiation was 1.8 W and the lamp had a wavelength spectrum of 300–410 nm with a maximum at 355 nm. The light intensity entering the reactor was determined by potassium ferrioxalate actinometry as described elsewhere [10].

In the immobilized system the catalyst was coated onto the outer wall of the inner tube by dipcoating (see below). Air was supplied through a glass mesh at the bottom of the reactor (Fig. 1), or through a sparger in the supply vessel. The total volume of the system was 650×10^{-6} m^3.

A Verder gear pump V540.05 was used for liquid circulation. In contrast, a Watson–Marlow 604U/R pump was used in the suspended system. Here, the total volume was 500×10^{-6} or 650×10^{-6} m^3. Air was supplied by a sparger present in the supply vessel.

2.2. Chemical substances

Degussa P-25 titanium dioxide was used as photocatalyst without further pretreatment. It has a BET surface of 55 m^2 g^{-1} and a particles size of 30 nm, which form agglomerates of 0.1–0.3 μm. Purified water (Millipore Milli-Q) was used to make the formic acid (reagent grade, Merck, 98–100%) solutions. Preliminary tests revealed that formic acid was not degraded by UV-A light alone. Only in the presence of both titanium dioxide and UV-A light, a rapid decrease in concentration was observed.

2.3. Analysis

Formic acid was analyzed off-line with capillary electrophoresis. A deactivated uncoated fused silica capillary with an internal diameter of 0.75 μm was used. The electrolytic solution was 4.6 mM chromate and 0.46 mM OFM-Anion-BT in Milli-Q water, where the pH was adjusted to 8 with sulfuric acid. Before use the electrolytic solution was vacuum filtrated over a 0.45 μm nylon filter for 10 min to remove air bubbles. Oxygen was analyzed on-line with an INGOLD oxygen electrode.

2.4. Catalyst immobilization

The catalyst was adhered onto the glass tube by dipcoating. The glass tube was thoroughly cleaned by ultrasonic rinsing with ethanol, dichloromethane, a mixture of $NH_3/H_2O_2/H_2O$ (1:1:5 v/v) and a mixture of HCl/H_2O (1:6 v/v). Between the different steps, the glass was thoroughly rinsed with Milli-Q water and afterwards dried for 1 h at 393 K. A 5% (w/w) suspension of titanium dioxide in water was prepared with Milli-Q water and ultrasonic mixing for 1 h. The glass tubes were dipped in the solution at a constant velocity of 1.3×10^{-3} m s^{-1} with a dipcoating apparatus as described elsewhere [11]. Between the dips the

layer was dried at room temperature for 10 min. The tubes with the immobilized catalyst were annealed by raising the temperature gradually with 3° per minute to avoid cracking of the layer, to a maximum temperature of 573 K at which it remained for 3 h. After this period the temperature was decreased with 5° per minute to room temperature. The total amount of catalyst on the tube was determined gravimetrically and varied from 0 to 3.6 g m^{-2}.

2.5. Experimental procedure

Prior to each experiment, the lamps were preheated for 30 min to obtain a constant light intensity. Before a tube with titanium dioxide was used for the first time, it was rinsed with Milli-Q water with the lamp turned on for 15 h to make sure that no pollutants were present on the catalyst surface. In the experiments with the suspended system, the titanium dioxide was ultrasonically suspended in Milli-Q water for 30 min just before the start of an experiment. Experiments with variable amounts of catalyst, various initial acid and oxygen concentrations and flows were performed. The temperature of the cooling water was 293 K and the Reynolds number, defined as $\rho v d/\eta$, in the system varied between 720 and 2400 corresponding to flows of $35 - 117 \times 10^{-6}$ m^3 s^{-1} (ρ is the density (kg m^{-3}), v the velocity in the reactor (m s^{-1}), d the hydraulic diameter (m) (defined as diameter of outer tube minus diameter of inner tube) and η the viscosity (Pa s)). The air flow in the immobilized system was 2.5×10^{-5} m^3 s^{-1}.

3. Results and discussion

3.1. Suspended system

With the suspended system it is important that all the catalyst reaches the illuminated zone in the reactor. Since, the penetration depth of the light in the fluid is small, the flow rate should be high enough to guarantee the necessary degree of mixing of the fluid in the reactor. Preliminary measurements with variable flow rates in the suspended system showed that the degradation of formic acid was independent of the flow rate, indicating that the catalyst could reach the illuminated zone in the reactor.

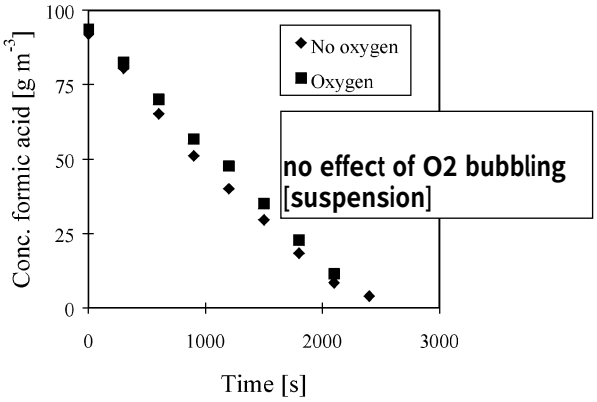

Fig. 2. The influence of oxygen addition on the degradation rate in the suspended catalyst system. $[TiO_2] = 500$ g m^{-3}, $V_{tot} = 650 \times 10^{-6}$ m^3, $Re = 1440$, $T = 293$ K.

The addition of oxygen had hardly any effect in the suspended system, see Fig. 2. The concentration of oxygen decreased to 60% of the maximum saturated concentration ($C_{max} = 9$ g m^{-3}) in case of no oxygen addition whereas the concentration decreased 2% with oxygen added to the system. From these results it can be concluded that oxygen is not deficient at the surface. Extra addition of oxygen does not increase the reaction rate by decreasing the recombination rate of the electrons and holes in the semiconductor. A possible explanation for the slight decrease in activity is that the catalyst is less efficiently illuminated due to bubbles in the suspension.

3.2. Modeling of the suspended system

In photocatalysis the degradation of pollutants is often described with the Langmuir–Hinshelwood kinetics [5]. For the recirculating batch system the mass balance of formic acid can then be written as

$$-\frac{dC}{dt} = \frac{k_r K_{ads} C}{1 + K_{ads} C} \frac{V_{reac}}{V_{tot}} \quad (1)$$

where C is the concentration of formic acid (g m^{-3}), t the reaction time (s), k_r the reaction rate constant (g m^{-3} s^{-1}), K_{ads} the Langmuir–Hinshelwood adsorption constant (m^3 g^{-1}), V_{reac} the volume of the reactor (m^3) and V_{tot} the total liquid volume in the recirculating batch system (m^3). Two asymptotic situations can

in suspension system
almost same slope --> zero-order kinetics

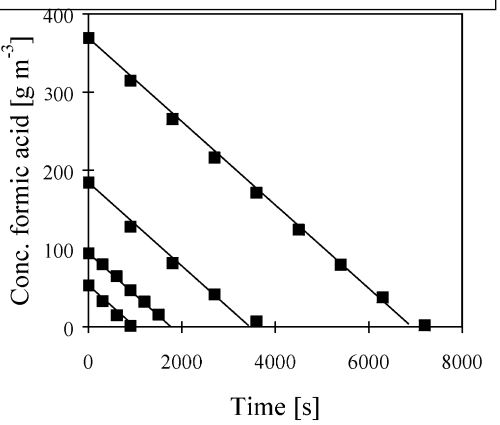

Fig. 3. The degradation of formic acid in the suspended catalyst system for various initial concentrations. Lines: pseudo 0th order model. $[TiO_2] = 250\,g\,m^{-3}$, $V_{tot} = 500 \times 10^{-6}\,m^3$, $Re = 1030$, $T = 293\,K$, no addition of oxygen.

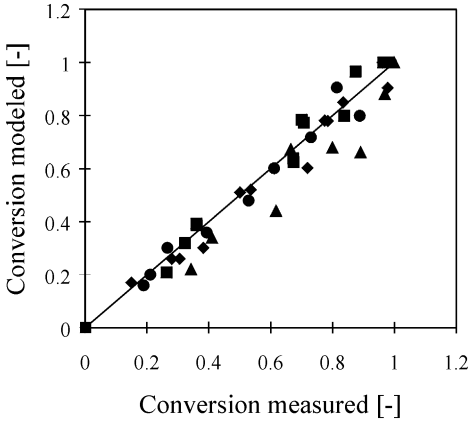

Fig. 4. Parity plot of the degradation in the suspended catalyst system, modeled with the pseudo 0th order model. Concentrations of TiO_2: (◆) $250\,g\,m^{-3}$, (■) $500\,g\,m^{-3}$, (●) $1000\,g\,m^{-3}$, (▲) $2000\,g\,m^{-3}$. Initial concentrations formic acid range: 50–$400\,g\,m^{-3}$.

be identified:

$$-\frac{dC}{dt} = k_r K_{ads} C \frac{V_{reac}}{V_{tot}} = k_1 C \frac{V_{reac}}{V_{tot}} \quad \text{for } 1 \gg K_{ads}C \text{ (pseudo 1st order)} \tag{2}$$

$$-\frac{dC}{dt} = k_r \frac{V_{reac}}{V_{tot}} = k_0 \frac{V_{reac}}{V_{tot}} \quad \text{for } 1 \ll K_{ads}C \text{ (pseudo 0th order)} \tag{3}$$

The degradation of formic acid was measured for various suspended catalyst concentrations (500–$2000\,g\,m^{-3}$). The degradation rate in the suspended system appeared to be successfully described by the pseudo 0th order model over a large concentration range, see Fig. 3. Slight deviation from the model for low concentration levels were observed which can be expected since then $K_{ads}C$ is probably no longer much larger than 1. The parity plot shown in Fig. 4 illustrates the ability of the pseudo 0th order model to describe the data obtained with the various catalyst concentrations applied.

The reaction rate constant shows a small increase with increasing catalyst loading from 0.5 to $2 \times 10^3\,g\,m^{-3}$, and seems to reach the maximum value for $2 \times 10^3\,g\,m^{-3}$ as has also been found by Aguado et al. [12], see Fig. 5.

3.3. Immobilized system

Immobilized systems often suffer from mass transfer limitation [8,9]. From experiments with variable flow rates, it was observed that the degradation rate of formic acid both with and without oxygen addition increased with increasing flow rate, indicating the presence of mass transfer limitation in our system as well, see Fig. 6. The shape of the curves shows that in this system the experiments cannot be described with the pseudo 0th order model. Due to the mass transfer limitation the surface concentration will be much lower,

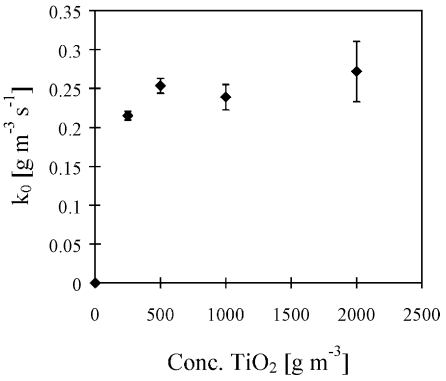

Fig. 5. Pseudo 0th order reaction rate constants with 95% confidence intervals.

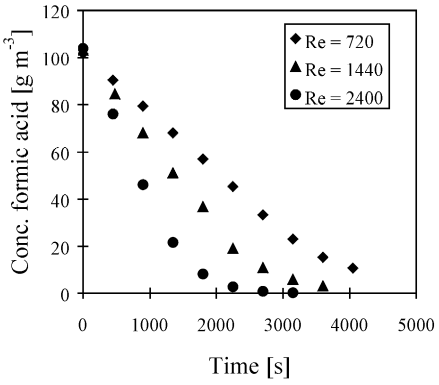

Fig. 6. The influence of the water flow rate on the degradation rate in the immobilized catalyst system with indirect oxygen addition in the reactor (one-phase in reactor). $W_{cat} = 3.6\,g\,m^{-2}$, $V_{tot} = 650 \times 10^{-6}\,m^3$, $T = 293\,K$.

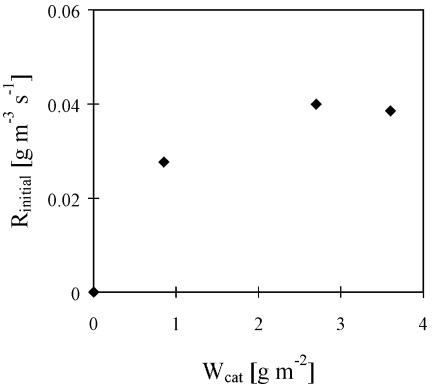

Fig. 8. The influence of the amount of catalyst on the initial degradation rate in the immobilized catalyst system, one-phase in reactor. $C_0 = 100\,g\,m^{-3}$, $V_{tot} = 650 \times 10^{-6}\,m^3$, $Re = 1440$, $T = 293\,K$.

causing the value of $K_{ads}C$ to be no longer much larger than 1. Therefore, the Langmuir–Hinshelwood kinetic model will describe these measurements as has also been found by Matthews [13] for the degradation of formic acid in an immobilized system.

Oxygen has a positive effect on the degradation rate in the immobilized catalyst system (Fig. 7). Oxygen acts as an electron scavenger, thus decreasing the recombination rate in the semiconductor [14]. The degradation rate in the system with oxygen bubbling through the reactor via a glass sieve (two-phases in reactor) is faster relative to that in the system with oxygen addition through a sparger in the supply vessel (one-phase in the reactor), see Fig. 7. Since the oxygen concentration remained the same during the experiments this difference appears to be caused by an increase of the mass transfer rate in the two-phase system. The mass transfer coefficient, k_l, is increased due to higher turbulence caused by the two-phase flow along the catalyst surface.

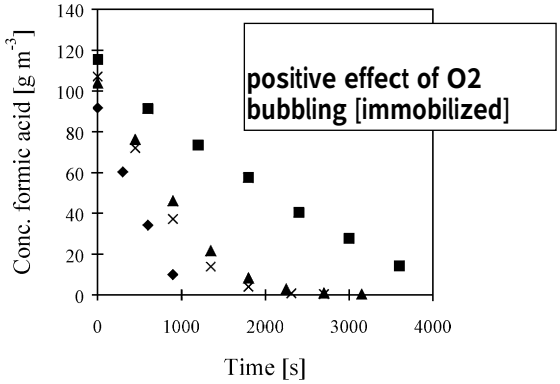

Fig. 7. The performance of the different systems: (◆) suspended catalyst system: $[TiO_2] = 2000\,g\,m^{-3}$, $V_{tot} = 500 \times 10^{-6}\,m^3$, $Re = 1030$, $T = 293\,K$, no addition of oxygen. (×) Immobilized system, addition of oxygen, two-phases in reactor: $W_{cat} = 3.6\,g\,m^{-2}$, $V_{tot} = 650 \times 10^{-6}\,m^3$, $Re = 2400$, $T = 293\,K$. (▲) Immobilized catalyst system, addition of oxygen, one-phase in reactor: $W_{cat} = 3.6\,g\,m^{-2}$, $V_{tot} = 650 \times 10^{-6}\,m^3$, $Re = 2400$, $T = 293\,K$. (■) Immobilized catalyst system, no addition of oxygen: $W_{cat} = 2.74\,g\,m^{-2}$, $V_{tot} = 285 \times 10^{-6}\,m^3$, $Re = 1030$, $T = 293\,K$.

With increasing amounts of catalyst coated on the tube the initial reaction rate increases until a maximum value is reached, see Fig. 8. This can be explained by an increased amount of light absorbed by the catalyst layer with an increasing layer thickness, until all the light falling on the catalyst will be absorbed and the maximum activity is reached. Also, mass transfer phenomena will influence the dependence of the reaction rate on the amount of catalyst, since mass transfer limitations will be more severe for higher reaction rates.

3.4. Suspended versus immobilized

For optimal comparison, the quantum yield, Φ, has been determined for the experiments depicted in Fig. 7. The quantum yield used here is defined as [2]

Table 1
Quantum yields of different systems[a]

	Slurry 2×10^3 g m^{-3}	Immobilized without O_2 addition	Immobilized O_2 addition one-phase in reactor	Immobilized O_2 addition two-phases in reactor
Specific area (m^2 m^{-3})[b]	10300	177[c]	177[c]	177[c]
Quantum yield (–)	0.28	0.063	0.22	0.28

[a] Quantum yields of experiments depicted in Fig. 7.
[b] $a_{sus} = 6C_{TiO_2}/\rho_{TiO_2}d_p$ with C_{TiO_2} is concentration catalyst (g m^{-3}), ρ_{TiO_2} is the density of titanium dioxide (g m^{-3}) and d_p is the diameter of the catalyst agglomerates (m). $a_{imm} = A_{cat}/V_{reac}$ with A_{cat} is the external catalyst area (m^2) [11].
[c] This value is actually higher, since the layer is porous.

$$\Phi = \frac{(dC_0/dt)V_{tot}}{I_0} \quad (4)$$

where dC_0/dt is the initial degradation rate (mol m^{-3} s^{-1}) and I_0 the amount of photons entering the reactor (Einstein s^{-1}). I_0 is equal for all three systems, because the same reactor and lamp were used. The value for I_0 was determined with actinometry as 4×10^{-6} Einstein s^{-1}.

In the two-phase system Φ is four times as high as that in the immobilized system without oxygen addition, see Table 1. In the suspended system Φ is comparable with that in the two-phase system, which is remarkable since the specific area is much larger in the suspended system. Due to the difference in kinetics (pseudo 0th order in suspended system versus Langmuir–Hinshelwood kinetics in immobilized system), the quantum yield in the immobilized system will decrease with initial concentration (dC_0/dt decreases), whereas in the suspended system it remains constant. The values for the quantum yield are comparable to values found for the degradation of formic acid by Sczechowski et al. [15].

Since, the quantum yield of the two-phase immobilized system is comparable to that of the suspended system and a costly separation step is necessary in the suspended system, an optimal reactor design for photocatalytic water purification will be an immobilized system optimized with respect to catalyst layer thickness, light intensity, specific area and mass transfer.

4. Conclusions

Formic acid can be easily degraded with heterogeneous photocatalysis. The degradation experiments in the suspended catalyst system can be very well modeled with the pseudo 0th order model. The activity of the suspended system reaches a maximum for 2×10^3 g m^{-3}. The addition of oxygen hardly affects the activity of the suspended system. The degradation experiments in the immobilized system show that mass transfer limitation occurs. Comparing the immobilized systems with and without oxygen addition, the system in which oxygen is introduced through a glass sieve in the bottom of the reactor appears to be more efficient, not only because oxygen acts as an efficient electron scavenger, but also due to increased mass transfer in this two-phase reactor. This immobilized system has a quantum yield which is comparable to that of the suspended system. Since the suspended system has the disadvantage of an expensive downstream separation step, it seems attractive to focus on the development of two-phase immobilized systems with maximum immobilized surface area per unit reactor volume and optimal light intensity and catalyst layer thickness.

Acknowledgements

This work was supported by the Netherlands Foundation for Chemical Research (SON) with financial aid from the Netherlands Technology Foundation. We like to thank Philips for their generous supply of UV lamps.

References

[1] O. Legrini, E. Oliveros, A.M. Braun, Photochemical processes for water treatment, Chem. Rev. 93 (1993) 671–698.
[2] M.R. Hoffmann, S.T. Martin, W. Choi, D.W. Bahnemann, Environmental applications of semiconductor photocatalysis, Chem. Rev. 95 (1995) 69–96.